Pardi, A., Walker, R., Rapoport, H., Wider, G., & Wuthrich, K. (1983a) *J. Am. Chem. Soc. 105*, 1652-1653.
Pardi, A., Morden, K. M., Patel, D. J., & Tinoco, I., Jr. (1983b) *Biochemistry 22*, 1107-1113.
Patel, D. J., Pardi, A., & Itakura, K. (1982a) *Science (Washington, D.C.) 216*, 581-590.
Patel, D. J., Kozlowski, S. A., Rice, J. A., Marky, L. A., Breslauer, K. J., Broka, C., & Itakura, K. (1982b) in *Topics in Nucleic Acid Structure* (Neidle, S., Ed.) Vol. 2, pp 81-136, MacMillan, London.
Patel, D. J., Kozlowski, S. A., Marky, L. A., Rice, J. A., Broka, C., Dallas, J., Itakura, K., & Breslauer, K. J. (1982c) *Biochemistry 21*, 437-444.
Patel, D. J., Kozlowski, S. A., Ikuta, S., & Itakura, K. (1984) *Fed. Proc., Fed. Am. Soc. Exp. Biol. 43*, 2663-2670.
Quigley, G. J., & Rich, A. (1976) *Science (Washington, D.C.) 194*, 796-806.
Rich, A., Nordheim, A., & Wang, A. H. (1984) *Annu. Rev. Biochem. 53*, 791-846.
Scheek, R. M., Boelens, R., Russo, N., van Boom, J. H., & Kaptein, R. (1984) *Biochemistry 23*, 1371-1376.
Schimmel, P. R., & Redfield, A. G. (1980) *Annu. Rev. Biophys. Bioeng. 9*, 181-221.
Tibanyenda, N., de Bruin, S. H., Haasnoot, C. A., van der Marel, G., van Boom, J. H., & Hilbers, C. W. (1984) *Eur. J. Biochem. 139*, 19-27.
Weiss, M. A., Patel, D. J., Sauer, R. T., & Karplus, M. (1984) *Proc. Natl. Acad. Sci. U.S.A. 81*, 130-134.
Wemmer, D. E., & Reid, B. R. (1985) *Annu. Rev. Phys. Chem. 36*, 105-137.
Williamson, M. P., Havel, T. F., & Wuthrich, K. (1985) *J. Mol. Biol. 182*, 295-315.
Zuiderweg, E. R., Scheek, R. M., Boelens, R., van Gunsteren, W., & Kaptein, R. (1985) *Biochimie 67*, 707-715.

Extrahelical Adenosine Stacks into Right-Handed DNA: Solution Conformation of the d(C-G-C-A-G-A-G-C-T-C-G-C-G) Duplex Deduced from Distance Geometry Analysis of Nuclear Overhauser Effect Spectra†

Dennis Hare
Infinity Systems, 14810 216th Avenue NE, Woodinville, Washington 98072
Lawrence Shapiro and Dinshaw J. Patel*
Department of Biochemistry and Molecular Biophysics, College of Physicians and Surgeons, Columbia University, New York, New York 10032

Received May 29, 1986; Revised Manuscript Received July 25, 1986

ABSTRACT: This paper reports on features of the three-dimensional structure of the d(C-G-C-A-G-A-G-C-T-C-G-C-G) self-complementary duplex (designated adenosine 13-mer), which contains symmetrical extrahelical adenosines in the interior of the helix. The majority of the protons have been assigned from two-dimensional nuclear Overhauser effect (NOESY) spectra of the adenosine 13-mer in H_2O and D_2O solution. The measurement of NOESY cross-peak volume integrals as a function of mixing time has yielded a set of 96 short (<4.5-Å) proton–proton distances defined by lower and upper bounds, which have served as input parameters for a distance geometry analysis of one symmetric half of the adenosine 13-mer duplex. We demonstrate that the extrahelical adenosine stacks into the duplex for all refined structures without disruption of base pairing on either side of the modification site. The distance geometry refinement yields two classes of conformations consistent with distance measurements but which differ in orientation of the stacked extrahelical adenosine at the modification site.

The conformation of DNA duplexes containing helical interruptions resulting from the presence of an unpaired base on one strand is of considerable interest in mechanisms of frame shift mutagenesis (Streisinger et al., 1966). The extrahelical base has the potential of either stacking into the duplex or looping out into solution so that addition or deletion mutations can result due to partial misalignment of strands during replication. The repair mechanisms are also governed by the conformation and stability of the extrahelical base at the helix interruption site in the interior of the duplex. Recent results on the role of aberrant nucleic acid conformations in frame shift mutagenesis have stressed the formation of extrahelical bases and mismatched base pairs in the stem of hairpin loops generated at DNA sequences containing quasipalindromic sites (Ripley, 1982; de Boer & Ripley, 1984).

Some structural features at extrahelical sites have been determined on the basis of analysis of one-dimensional NMR chemical shift and distance dependent nuclear Overhauser effect (NOE) parameters. Thus, it has been shown that the extrahelical adenosine stacks into the self-complementary d(C-G-C-A-G-A-A-T-T-C-G-C-G) duplex (Patel et al., 1982). Hydrogen exchange measurements at the individual base pair level demonstrate that stacking of the extrahelical adenosine results in faster hydrogen exchange rates and higher activation barriers at the flanking, as well as more distant, base pairs (Pardi et al., 1982). The thermodynamics and kinetics of the

† The research was supported by National Institutes of Health Grants GM 34504-02 to D.J.P. and GM 35620-02 to D.H. The NMR spectrometers were purchased from funds donated by the Robert Woods Johnson, Jr., Trust and the Matheson Trust toward setting up the NMR Center in the Basic Medical Sciences at Columbia University.

0006-2960/86/0425-7456$01.50/0

Chart I

C1 – G2 – C3 – A4 – G5 – A6 – G7 – C8 – T9 – C10 —— G11 – C12 – G13

G13 – C12 – G11 —— C10 – T9 – C8 – G7 – A6 – G5 – A4 – C3 – G2 – C1

helix to coil transition of this extrahelical adenosine containing tridecanucleotide have been characterized by calorimetric (Patel et al., 1982) and temperature-jump (Chu & Tinoco, 1983) measurements, respectively.

By contrast, one-dimensional NMR chemical shift and NOE measurements demonstrate that the extrahelical cytidine loops out of the complementary d(CA_3CA_3G)·d(CT_6G) duplex (Morden et al., 1983). It has been shown further that the intercalator ethidium binds more strongly to this complementary oligonucleotide duplex containing a looped out cytidine than to the corresponding regular oligonucleotide duplex (Nelson & Tinoco, 1986).

There are no X-ray structures available on extrahelical base containing duplexes in the crystalline state through crystallization of the d(C-G-C-A-G-A-A-T-T-C-G-C-G) duplex has been reported recently (Saper et al., 1986). It was therefore of interest to determine the solution conformation of such duplexes by a distance geometry analysis of experimental interproton distances evaluated from two-dimensional nuclear Overhauser effect measurements. We report below on such a study which defines the conformation of the self-complementary d(C-G-C-A-G-A-G-C-T-C-G-C-G) duplex (designated adenosine 13-mer, Chart I) in aqueous solution.

Experimental Procedures

The d(C-G-C-A-G-A-G-C-T-C-G-C-G) adenosine 13-mer duplex was synthesized by Pharmacia P-L Biochemicals. The NMR spectrum confirmed the purity of the sample. The NMR sample was made up by dissolving 400 A_{260} units of adenosine 13-mer in 0.4 mL of 0.1 M NaCl, 10 mM phosphate, and 1 mM ethylenediaminetetraacetic acid (EDTA) buffer for recording NMR spectra in D_2O and H_2O solution.

We have outlined procedures for two-dimensional NMR data collection and processing, as well as measurements of distance constraints from NOE cross-peaks and their analysis by distance geometry algorithms in the previous paper on the 12-mer GT duplex (Hare et al., 1986). The same procedures were used in the present study of the adenosine 13-mer duplex.

Results

The numbering system for the self-complementary adenosine 13-mer is outlined in Chart I and applies for both spectral assignments and distance geometry analysis.

The adenosine 13-mer under study in this paper (Chart I) contains a central AGCT segment that replaces the central AATT segment in the adenosine 13-mer studied previously (Patel et al., 1982). This change was introduced in order to raise the helix–coil transition midpoint by replacing two A·T base pairs by two G·C base pairs in the center of the helix.

Exchangeable Proton Assignments. The imino proton spectrum of the adenosine 13-mer in 0.1 M NaCl, in H_2O at 5 °C, exhibits five nonterminal Watson–Crick base pairs in this duplex at low temperature. We have assigned these imino protons by monitoring the sequential line width changes with increasing temperature and from one- and two-dimensional nuclear Overhauser effect measurements.

A contour plot of the magnitude two-dimensional nuclear Overhauser effect (NOESY) spectrum of the adenosine 13-mer in H_2O at 5 °C is plotted between 6.5 and 14.0 ppm in Figure 1. We observe NOEs among the imino protons and between the imino protons (12.5–14.0 ppm) and the cytidine amino and adenosine H2 protons (7.4–8.6 ppm). We have recorded one-dimensional slices through two of these imino proton resonances, and these are plotted in Figure 2. The lowest field imino proton at 13.76 ppm is assigned to the imino proton of T9 and exhibits a strong intra base pair NOE to the

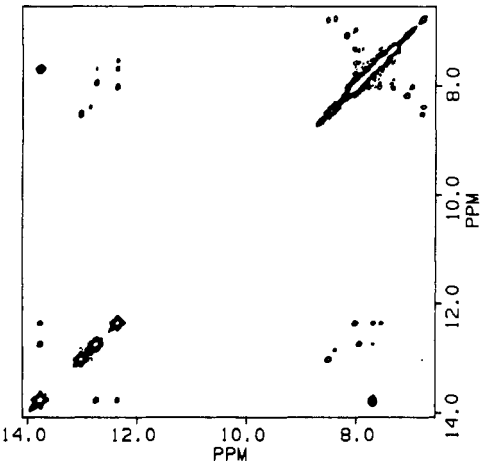

FIGURE 1: Magnitude NOESY spectrum (mixing time, 120 ms) of the adenosine 13-mer in 0.1 M NaCl and 10 mM phosphate, in H_2O at 5 °C.

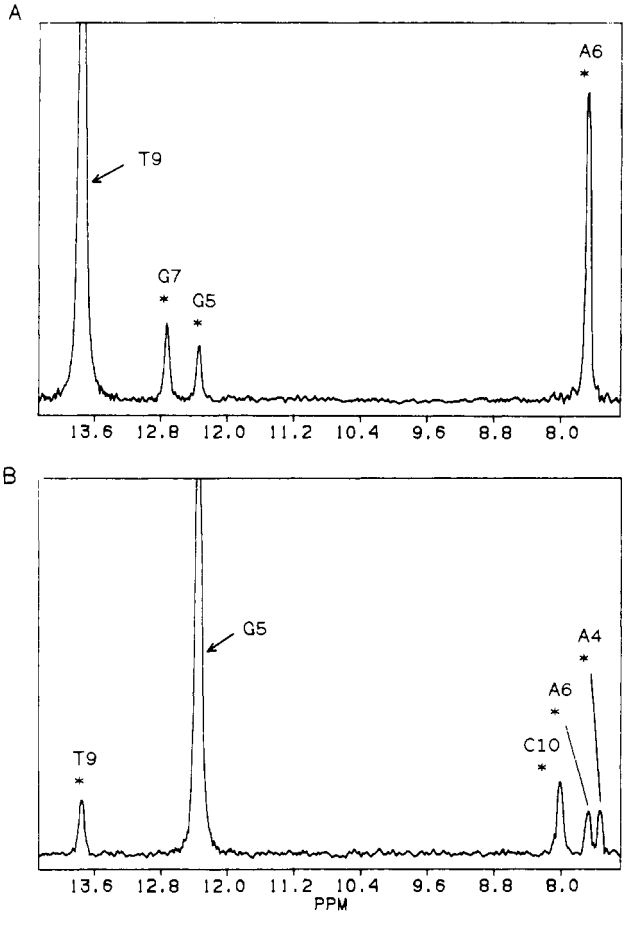

FIGURE 2: (A) One-dimensional NOE slice (7.0–14.0 ppm) establishing distance connectivities from the 13.76 ppm imino proton of T9 to the 7.69 ppm H2 proton of A6 in the same A6·T9 base pair and to the 12.74 and 12.36 ppm imino protons of flanking G7·C8 and G5·C10 base pairs, respectively. (B) One-dimensional NOESY slice (7.0–14.0 ppm) establishing distance connectivities from the 12.36 ppm imino proton of G5 to the 8.02 ppm hydrogen-bonded amino proton of C10 in the same G5·C10 base pair, as well as to the 13.76 ppm thymidine imino and 7.69 ppm adenosine H2 protons of the adjacent A6·T9 base pair and to the 7.54 ppm adenosine H2 of the adjacent extrahelical A4.

Table I: Proton Chemical Shifts of Nonterminal Imino, Cytidine Amino, and Adenosine H2 Protons in the Adenosine 13-mer Self-Complementary Duplex in 0.1 M NaCl, in H_2O at 5 °C

	chemical shift (ppm)			
	H1	H3	H4[a]	H2
G2·C12	13.03		8.51	
C3·G11	12.85		8.39	
G5·C10	12.36		8.02	
A6·T9		13.76		7.69
G7·C8	12.74		7.94	
A4				7.54

[a] Chemical shift is for hydrogen-bonded cytidine H4 amino proton.

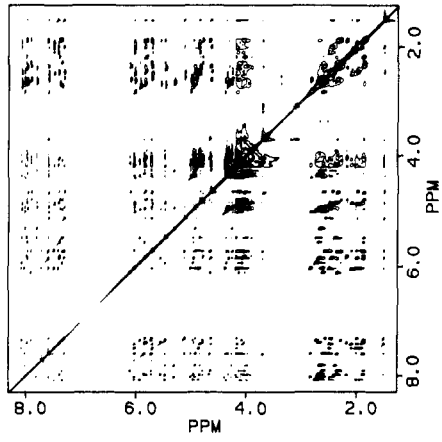

FIGURE 3: Phase-sensitive NOESY spectrum (mixing time, 250 ms) of the adenosine 13-mer in 0.1 M NaCl and 10 mM phosphate, in D_2O and 25 °C.

7.69 ppm adenosine H2 proton in its own A6·T9 base pair, as well as NOEs to the imino protons of flanking G5·C10 (12.36 ppm) and G7·C8 (12.74 ppm) base pairs (Figure 2A). We have searched for NOEs between the H2 proton on the extrahelical adenosine A4 and the imino protons of flanking G5·C10 and C3·G11 base pairs. The 12.85 ppm G11 imino proton exhibits an NOE to its own 8.39 ppm C3 hydrogen-bonded amino proton in the C3·G11 base pair. The 12.36 ppm G5 imino proton exhibits an NOE to its own 8.02 ppm C10 hydrogen-bonded amino proton in the G5·C10 base pair, as well as to the 7.69 ppm adenosine H2 proton of the flanking A6·T9 base pair and the 7.54 ppm adenosine H2 proton of the flanking A4 extrahelical base (Figure 2B). This latter NOE is critical since it establishes that the adenosine H2 proton of extrahelical A4 is within 4.5 Å of the imino proton of the adjacent G5·C10 base pair.

The guanosine and thymidine imino, cytidine amino, and adenosine H2 proton chemical shifts in the adenosine 13-mer at 5 °C are listed in Table I.

Nonexchangeable Proton Assignments. We have assigned the nonexchangeable base and sugar H1′, H2′, H2″, and H3′ protons in the adenosine 13-mer duplex in 0.1 M NaCl, in D_2O at 25 °C, from an analysis of the 250-ms mixing time NOESY spectrum presented as a contour plot in Figure 3. The cross-peaks are unusually well resolved as demonstrated from the expanded contour plots linking the base protons (7.2–8.2 ppm) with the sugar H1′ and cytidine H5 protons (5.0–6.2 ppm) and with the sugar H3′ protons (4.6–5.2 ppm) in panels A and B, respectively, of Figure 4.

Since the purpose of this study is structure determination, it is not reasonable to assume anything about the structure of this molecule that is not based on experimental data or implicit in its primary chemical structure. We expect, for example, to see an NOE from each purine H8 and pyrimidine

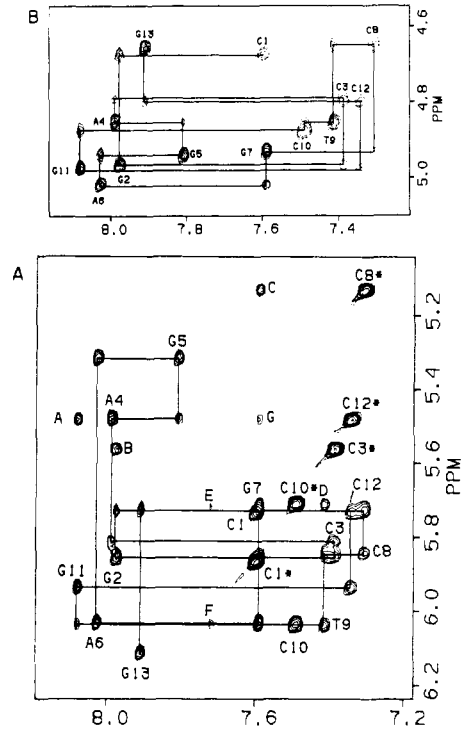

FIGURE 4: Expanded contour plots of phase-sensitive NOESY spectra (mixing time, 250 ms) of the adenosine 13-mer duplex in 0.1 M NaCl and 10 mM phosphate, in D_2O at 25 °C, establishing distance connectivities between (A) the base protons (7.2–8.2 ppm) and the sugar H1′ and cytidine H5 protons (5.0–6.2 ppm) and (B) the base protons (7.2–8.2 ppm) and the sugar H3′ protons (4.6–5.1 ppm). The lines follow the connectivities between adjacent base protons through their intervening sugar protons. The cytidine H5–H6 cross-peaks are designated by asterisks. The cross-peaks A–F are discussed in the text.

H6 to the H1′ proton of its own deoxyribose, since the chemical structure implies that this distance cannot exceed about 3.9 Å. Although most of these aromatic protons exhibit NOEs to two H1′ protons, one must assign these resonances from a combination of sequence information, structural information, and elimination. In the case of this oligomer, we found that the observed NOEs did agree with those for right-handed DNA (Hare et al., 1983; Scheek et al., 1984, Weiss et al., 1984), but this was a result of experimental data, not an initial assumption. We wish to stress that the NOE connectivities between the base protons and their own and 5′-flanking sugar H1′ protons can be monitored through the C3-A4-G5 segment, which includes the extrahelical adenosine that lacks a base on the partner strand (Figure 4A).

The observed NOEs between the purine H8 and pyrimidine H5 protons in the purine–(3′–5′)–pyrimidine G2–C3 step (peak B, Figure 4), the G7–C8 step (peak C, Figure 4), and the G11–C12 step (peak A, Figure 4) are consistent with a right-handed helix for the adenosine 13-mer duplex in solution.

We have analyzed in detail the 250-ms mixing time phase-sensitive NOESY spectrum (Figure 3) and the magnitude correlated (COSY) spectrum of the adenosine 13-mer duplex to confirm the above base and sugar H1′ and H3′ assignments and in addition establish the sugar H2′ and H2″ assignments. These nonexchangeable proton chemical shifts in the adenosine 13-mer at 25 °C are listed in Table II.

Distance Constraints—Nonexchangeable Protons. The NOESY spectra of the adenosine 13-mer at 25 °C have been recorded at mixing times of 50, 75, 100, 150, and 250 ms. The volume integrals of the assigned NOE crosspeaks as a function of mixing time yield approximate proton–proton distances

Table II: Nonexchangeable Proton Chemical Shifts of the Adenosine 13-mer Duplex in 0.1 M NaCl and 10 mM Phosphate, in D_2O at 25 °C

	chemical shift (ppm)						
	H8	H2	H6	H5/CH_3	H1′	H2′, H2″	H3′
C1			7.60	5.86	5.73	1.89, 2.36	4.68
G2	7.98				5.85	2.69, 2.69	4.97
C3			7.40	5.56	5.81	1.88, 2.19	4.79
A4	7.99	7.59			5.49	2.38, 2.38	4.85
G5	7.81				5.32	2.66, 2.66	4.94
A6	8.03	7.72			6.03	2.84, 2.84	5.02
G7	7.59				5.72	2.49, 2.58	4.93
C8			7.32	5.13	5.84	2.00, 2.46	4.65
T9			7.42	1.51	6.04	2.11, 2.49	4.86
C10			7.49	5.71	6.04	1.95, 2.02	4.87
G11	8.08				5.94	2.74, 2.74	4.98
C12			7.35	5.49	5.72	1.88, 2.30	4.80
G13	7.91				6.11	2.36, 2.61	4.65

Table III: Intranucleotide Nonexchangeable Proton Distance Constraints (in Angstroms) in the Adenosine 13-mer Duplex

	H1′–H8/H6	H2′–H8/H6	H2″–H8/H6	H3′–H8/H6	H1′–H2′	H1′–H2″	H1′–H2
C1		1.95–2.3	2.95–3.2	4.0–5.0		2.0–2.2	
G2	3.45–4.0			3.9–4.4			
C3	2.9–3.7	1.9–2.2	2.7–3.2	4.0–6.0	2.2–2.7	2.0–2.2	
A4	3.3–3.8			3.9–4.4			4.2–5.0
G5	3.6–4.05			3.9–4.5			
A6	3.7–4.5		2.4–2.7	3.6–4.0	2.2–2.7	2.0–2.2	
G7		2.1–2.35	2.4–2.7	3.5–4.2	2.2–2.7	2.1–2.4	
C8	3.7–4.1	2.2–2.5	2.5–3.1	3.8–4.4	2.35–2.70	1.95–2.15	
T9	3.4–4.0	2.0–2.2	2.3–2.7	3.7–4.2	2.3–2.6	1.9–2.2	
C10		1.9–2.2	2.0–2.5		2.5–2.8	2.0–2.25	
G11	3.6–4.3			3.5–3.9			
C12	3.0–3.8	1.9–2.3	2.5–2.8	4.0–6.0		2.1–2.4	
G13	3.5–3.8	2.0–2.3	2.4–3.1	3.8–4.3	2.1–2.7	1.9–2.1	

Table IV: Nonexchangeable Proton Distance Constraints (in Angstroms) between Adjacent Nucleotides in the Adenosine 13-mer Duplex

	H1′–H8/H6	H2″–H8/H6	H3′–H8/H6	H8/H6–H5/CH_3	H8/H6–H8/H6	H1′–H5	H2–H1′
C1–G2	3.7–4.7		4.0–5.5				
G2–C3	3.0–3.7		4.5–6.0	3.5–3.9	4.15–4.55	3.4–5.0	
C3–A4	3.7–4.5	2.5–3.5	4.5–6.0				
A4–G5	3.7–4.6		4.2–6.0				
G5–A6	2.9–3.3		3.8–5.0		4.3–5.3		
A6–G7	3.2–3.6		4.0–5.5		4.0–5.0		4.0–5.0
C8–T9	3.2–3.7	2.0–2.7					
T9–C10		2.0–2.7		2.8–3.7		3.4–5.0	
C10–G11	3.8–4.8		4.0–5.5				
G11–C12	2.9–3.3		4.0–6.0	3.6–4.0	3.95–4.35	3.4–5.0	
C12–G13	3.6–5.0	2.5–3.3	4.2–5.5				

defined by lower and upper bounds. The choice of the fixed distance yardsticks to measure the experimental distances has been discussed in the preceding paper (Hare et al., 1986). These proton–proton distance estimates within a nucleotide and between adjacent nucleotides for one symmetrical half of the adenosine 13-mer duplex at 25 °C are listed in Tables III and IV, respectively.

Distance Constraints—Exchangeable Protons. We have also estimated the distance constraints between imino protons and flanking base pair imino and adenosine H2 protons in the 120-ms mixing time NOESY spectrum of the adenosine 13-mer duplex at 5 °C. These values between protons on the same strand and between protons on partner strands are listed in Table V, and we assume that these distances remain within the defined bounds on raising the temperature to 25 °C.

Distance Geometry. The experimental distances and distance information inferred from chemical structure (bond distance and bond angles in distance form) were used as input parameters for the distance geometry algorithm. A starting embedded structure and the corresponding refined structure of one symmetrical half of the adenosine 13-mer are plotted as stereopairs in the top and bottom panels, respectively, of Figure 5. The extra adenosine is stacked into the helix in this adenosine 13-mer refinement designated G.

Table V: Exchangeable Proton Distance Constraints (in Angstroms) between Adjacent Nucleotides in the Adenosine 13-mer Duplex

	same strand	partner strands	
	H1/H3–H2	H1/H3–H1/H3	H1/H3–H2
G5–T9		3.6–3.9	
G7–T9		3.45–3.85	
G7–A6	4.15–4.45		
G5–A6	3.8–4.1		
G5–A4	3.8–4.2		
G11–A4			4.0–5.0

The algorithm was used to generate several different starting structures from the input distances and then to refine each of the structures until it agreed with all the input distance information. The refined structures yielded two classes of conformations that satisfied the distance constraints but differ in the orientation of the stacked extrahelical adenosine at the modification site in the adenosine 13-mer duplex.

Refined structures designated B (Figure 6, top) and G (Figure 6, bottom) belong to the first class, in which the stacked adenosine base is roughly parallel to the planes of the flanking base pairs. The interproton distance between the

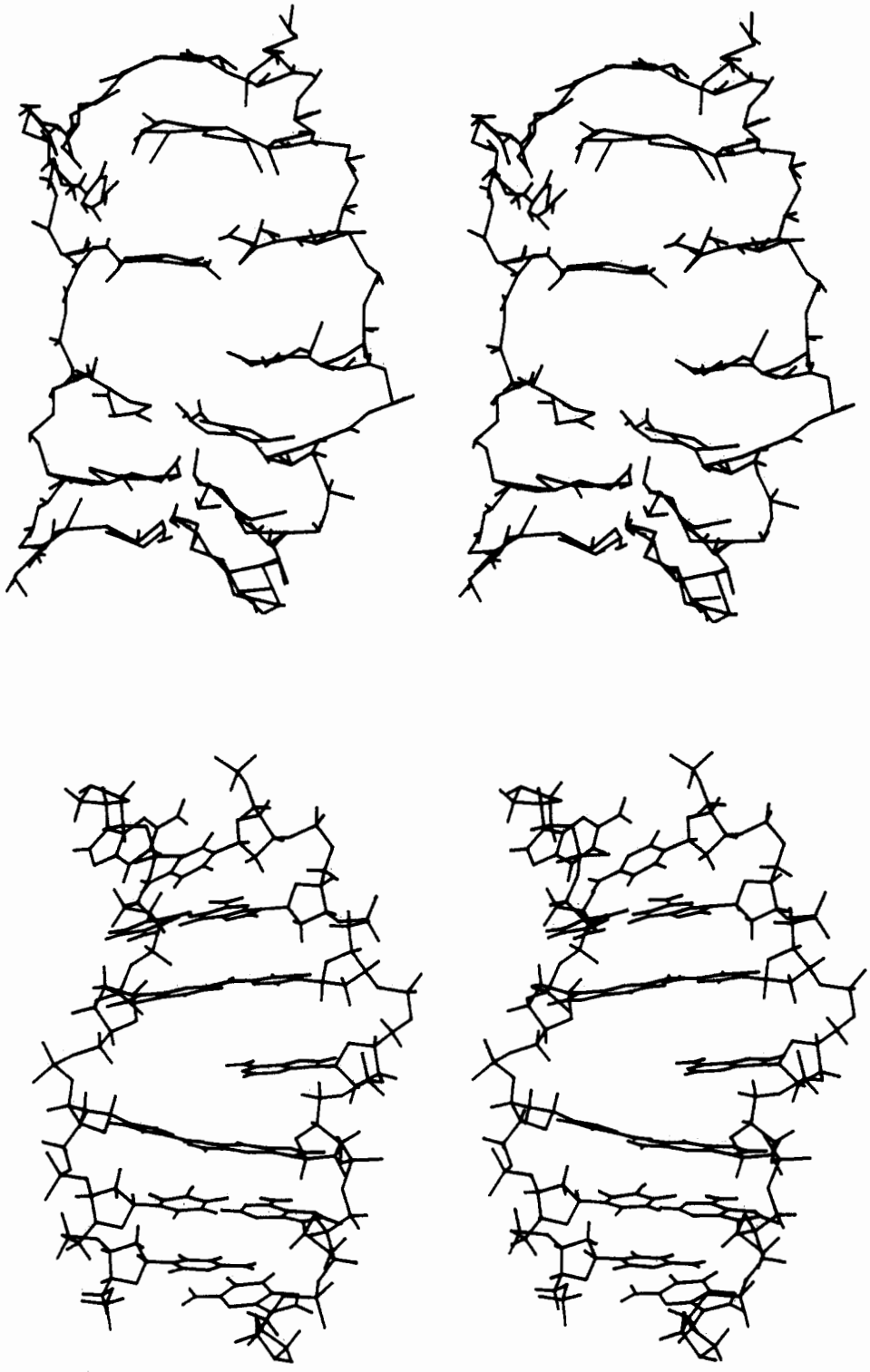

FIGURE 5: Stereopairs (top) of an initial embedded structure and (bottom) of the refined structure of one symmetrical half of the adenosine 13-mer duplex. These views correspond to the refinement designated G. The chain runs C1-G2-C3-A4-G5-A6-G7 from top to bottom of right strand, and the chain runs C8-T9-C10-G11-C12-G13 from bottom to top of left strand in stereopair.

guanosine imino proton of G5·C10 and the adenosine H2 of the stacked base A4 is 4.2 Å.

Refined structures designated A (Figure 7, top) and K (Figure 7, bottom) belong to the second class, in which the stacked adenosine base is twisted relative to the planes of the flanking base pairs. The interproton distance between the guanosine imino proton of G5·C10 and the adenosine H2 of the stacked A4 is 3.8 Å.

Side stereoviews of the refined structure G (Figure 8, top) and refined structure K (Figure 8, bottom) of the adenosine 13-mer duplex demonstrate that the extra adenosine is parallel to flanking base pairs for structure G belonging to the first class while it is no longer parallel at the modification site for structure K belonging to the second class.

Comparison of Refined Structures. We have compared refined structures by plotting the average difference in angstroms for atoms separated by an average distance $d \pm 0.5$ Å between pairs of adenosine 13-mer duplex refinements (Figure 9A). The average difference is much smaller between refined pairs B and G belonging to the first class of structures

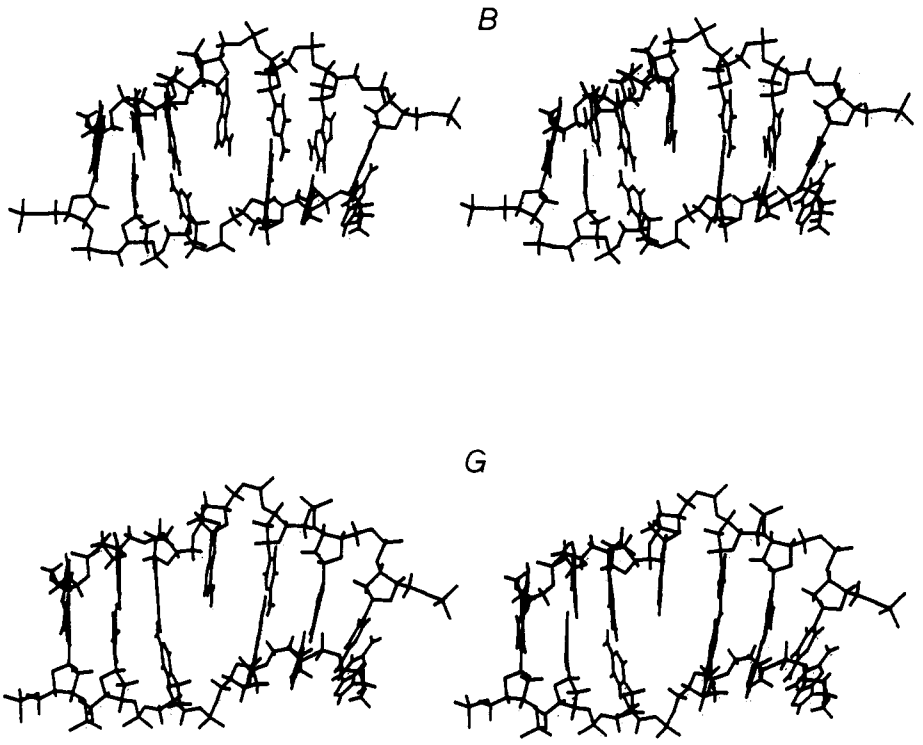

FIGURE 6: Stereopairs of refined structures B and G of one symmetrical half of the adenosine 13-mer duplex.

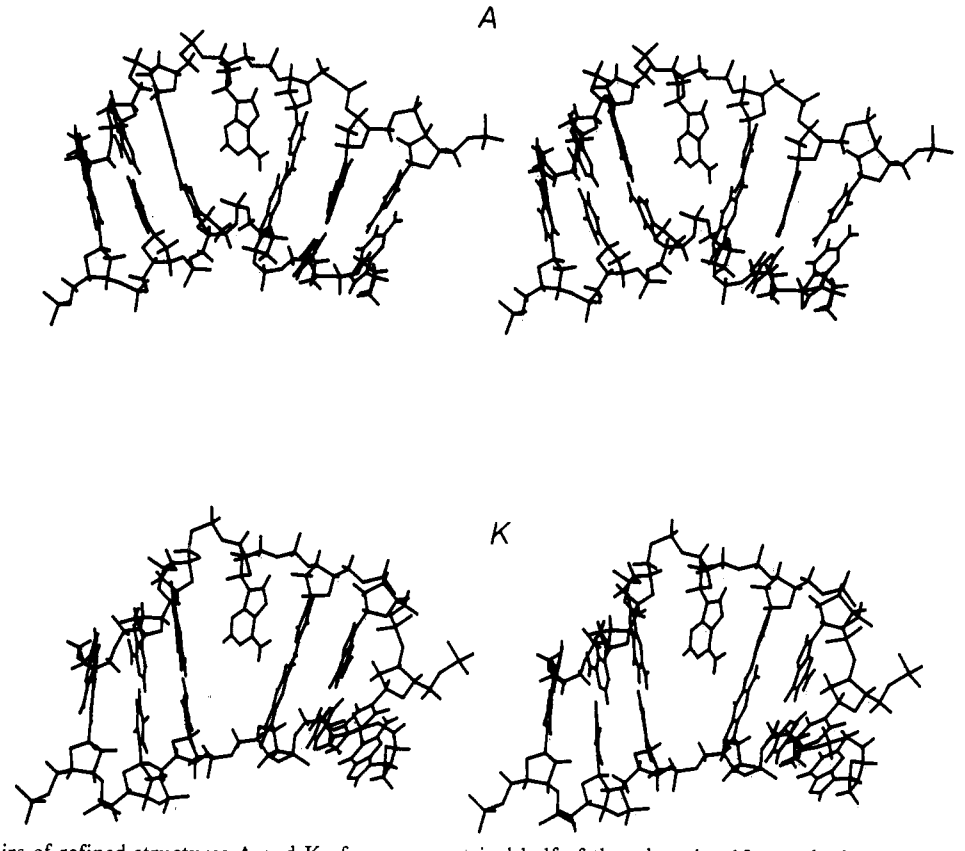

FIGURE 7: Stereopairs of refined structures A and K of one symmetrical half of the adenosine 13-mer duplex.

than between refined pairs A and K belonging to the second class of structures (Figure 9A). A similar trend is observed in a plot of the average coordinate difference in angstroms against residue number for the adenosine 13-mer duplex (Figure 9B).

Torsion Angles. We have plotted the glycosidic torsion angles and the sugar pucker pseudorotation angles at individual residues for the refined pairs B and G (Figure 10A) and for the refined pairs A and K (Figure 10B) in the adenosine 13-mer duplex. The majority of the glycosidic torsion angles are centered about 270° while the sugar ring pseudorotation angles are centered about 150° (Figure 10).

DISCUSSION

Spectral Assignments. The two-dimensional NOESY spectra are unusually well resolved for the adenosine 13-mer

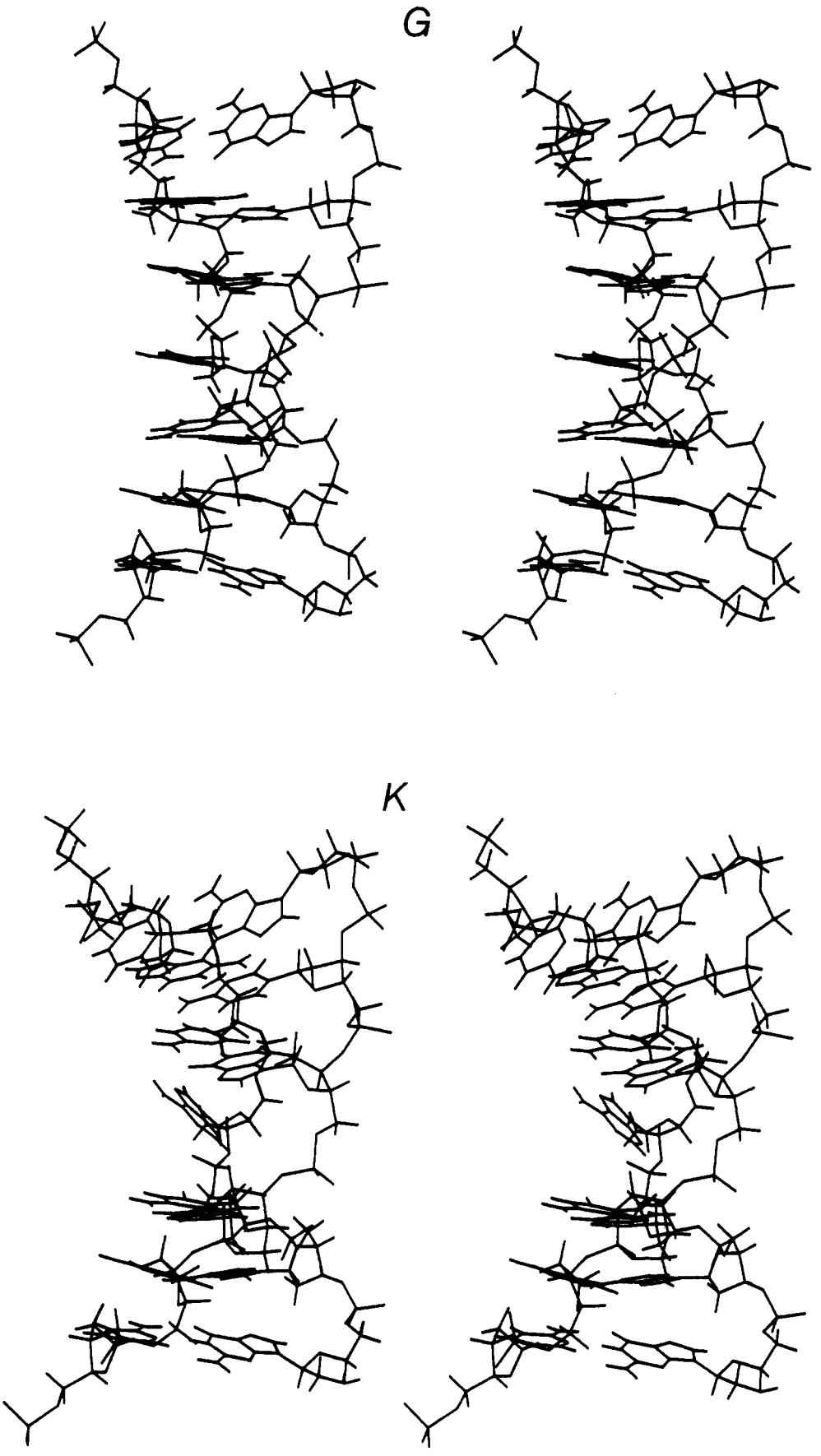

FIGURE 8: Stereopairs of refined structures G and K of one symmetrical half of the adenosine 13-mer duplex. This view is rotated 90° along the helix axis to emphasize the double-helical nature of the duplex and to stress the difference in bending between the two classes of refined structures.

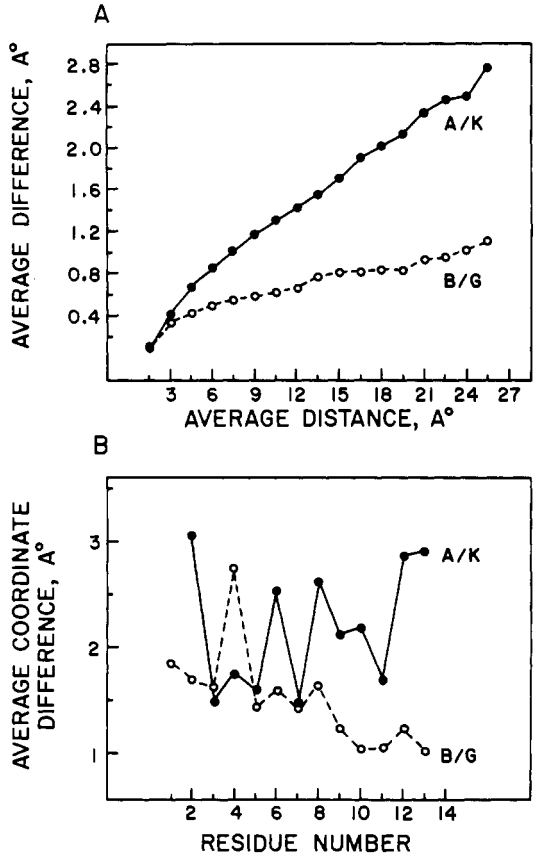

FIGURE 9: (A) Comparison of the average difference in angstroms for atoms separated by an average distance $d \pm 0.5$ Å between pairs of refined structures of the adenosine 13-mer duplex. The comparison was undertaken for pairs A and K and for pairs B and G. (B) Comparison of the average coordinate difference in angstroms for all atoms of a given residue between pairs of refined structures of the 12-mer GT duplex.

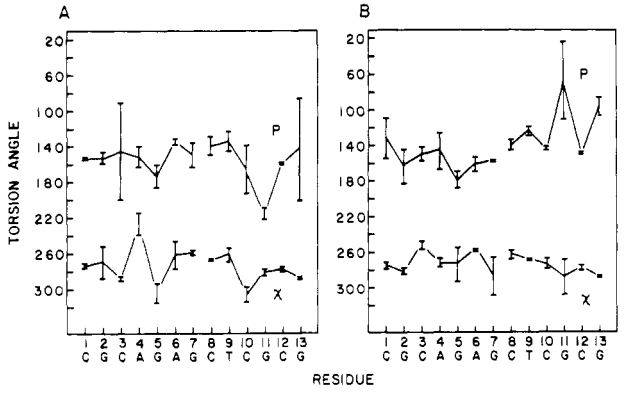

FIGURE 10: Plot of the lower and upper ranges for the glycosidic torsion angle χ and the sugar pucker pseudorotation value P at individual residue positions in the adenosine 13-mer refinements. (A) Plots based on refinements B and G. (B) Plots based on refinements A and K.

in H_2O solution at 5 °C (Figure 1) and in D_2O at 25 °C (Figure 3) so that it has been straightforward to assign the cross-peaks to yield the base and sugar H1′, H2′, H2″, and H3′ proton chemical shifts listed in Tables I and II.

Distance Constraints. The observed thymidine imino to adenosine H2 and guanosine imino to cytidine amino NOEs (Figure 1) demonstrate that A·T and G·C base pairing is intact in the adenosine 13-mer at 5 °C. These hydrogen bonding constraints are important for linking the two strands with each other.

We have listed the 96 proton–proton distance constrains for one symmetrical half of the adenosine 13-mer defined by lower and upper bounds in Tables III–V. These include distances between nonexchangeable base protons (Table IV), between imino protons (Table V), and between imino and adenosine H2 protons (Table V) on adjacent base pairs. Such constraints are observed between adjacent bases on the same strand (Table IV) and between strands (Table V), thus orienting the two stands in the duplex.

The observed NOE between the imino proton of G5·C10 and the extrahelical adenosine H2 proton (Figures 1 and 2B) unequivocally demonstrates that the extrahelical adenosine stacks into the duplex rather than looping out into solution.

Refined Structures. The extra adenosine was stacked into the duplex in all refined structures. Two classes of refined structures are observed differing in the orientation of the stacked adenosine with flanking dG·dC base pairs. We observe smaller differences on comparison of refined pairs B and G for which the extra adenosine is parallel to the flanking base pairs in contrast to pairs A and K for which the adenosine is partly twisted relative to the planes of flanking base pairs (Figure 9). We therefore favor the class of refinements represented by B and G (Figure 6) over those represented by A and K (Figure 7) for the structure of the adenosine 13-mer duplex in solution. The two classes of refined structures observed for the adenosine 13-mer in solution may reflect the fact that the constraints on the extra adenosine are rather loose and allow considerable conformational freedom. It is quite possible that the molecule is relatively flexible at the stacked extra adenosine due to lack of hydrogen bonding interactions.

The glycosidic torsion angles and sugar puckers are centered about their B-DNA values for refinements B and G (Figure 10A) and for refinements A and K (Figure 10B) for the adenosine 13-mer in solution. We do note that, for refined structures B and G, the glycosidic torsion angle at extra adenosine A4 has a value of 230°, which is intermediate between the B-DNA (257°) and A-DNA (201°) values (Figure 9A).

We wish to stress that the present combination of NMR and distance geometry methods provides structural information on base pair stacking, glycosidic torsion angle, and sugar pucker but is unable to define the sugar–phosphate backbone C3′–O3′–P–O5′–C5′–C4′ torsion angles for the adenosine 13-mer duplex in solution.

Registry No. A, 58-61-7; adenosine 13-mer, 104598-27-8.

REFERENCES

Chu, Y. G., & Tinoco, I., Jr. (1983) *Biopolymers 22*, 1235–1246.

De Boer, J. G., & Ripley, L. S. (1984) *Proc. Natl. Acad. Sci. U.S.A. 81*, 5528–5531.

Hare, D. R., Wemmer, D. E., Chou, S. H., Drobny, G., & Reid, B. R. (1983) *J. Mol. Biol. 171*, 319–336.

Hare, D., Shapiro, L., & Patel, D. J. (1986) *Biochemistry* (preceding paper in this issue).

Morden, K. M., Chu, Y. G., Martin, F. H., & Tinoco, I., Jr. (1983) *Biochemistry 22*, 5557–5563.

Nelson, J. W., & Tinoco, I., Jr. (1985) *Biochemistry 24*, 6416–6423.

Pardi, A., Morden, K. M., Patel, D. J., & Tinoco, I., Jr. (1982) *Biochemistry 21*, 6567–6574.

Patel, D. J., Kozlowski, S. A., Marky, L. A., Rice, J. A., Broka, C., Itakura, K., & Breslauer, K. J. (1982) *Biochemistry 21*, 445–451.

Ripley, L. S. (1982) *Proc. Natl. Acad. Sci. U.S.A. 79*, 4128–4132.

Saper, M. A., Eldar, H., Mizuuchi, K., Nickol, J., Apella, E.,

& Sussman, J. L. (1986) *J. Mol. Biol. 188*, 111-113.
Scheek, R. M., Boelens, R., Russo, N., van Boom, J. H., & Kaptein, R. (1984) *Biochemistry 23*, 1371-1376.
Streisinger, G., Okada, Y., Emrich, J., Newton, J., Tsugita, A., Terzaghi, E., & Inouye, M. (1966) *Cold Spring Harbor Symp. Quant. Biol. 31*, 77-84.
Weiss, M. A., Patel, D. J., Sauer, R. T., & Karplus, M. (1984) *Proc. Natl. Acad. Sci. U.S.A. 81*, 130-134.

Conversions of Poly(2-aminodeoxyadenylate-5-halodeoxyuridylate) from B to A Forms in High Salt. An NMR and Circular Dichroism Study

Babul Borah,[‡] Frank B. Howard,[§] H. Todd Miles,[§] and Jack S. Cohen*[,‡]

Clinical Pharmacology Branch, Division of Cancer Treatment, National Cancer Institute, National Institutes of Health, Bethesda, Maryland 20205, and Laboratory of Molecular Biology, National Institute of Arthritis, Diabetes and Digestive and Kidney Diseases, National Institutes of Health, Bethesda, Maryland 20892

Received May 6, 1986; Revised Manuscript Received August 6, 1986

ABSTRACT: Proton one- and two-dimensional nuclear Overhauser enhancement (1D and 2D NOE) spectroscopy has been used to demonstrate that poly(d2NH$_2$A-d5IU) and poly(d2NH$_2$A-d5BrU) are converted from the B to the A conformation in high salt, as found previously for poly(d2NH$_2$A-dT) [Borah, B., Cohen, J. S., Howard, F. B., & Miles, H. T. (1985) *Biochemistry 24*, 7456-7462]. The 2D NOE and 1D NOE spectra exhibit strong base proton (H8,H6)-H3′ cross relaxation, suggesting short interproton distances. These results are indicative of a C3′-endo sugar pucker for both purine and pyrimidine residues in an A or closely related structure. The circular dichroism and UV spectra are consistent with the interpretation of an A conformation in high salt.

The conformational equilibrium between right-handed B-DNA and left-handed Z-DNA depends on several extrinsic and intrinsic factors. The level of hydration, ionic strength, temperature, specific ligands, and supercoiling are extrinsic factors that may influence the B-Z equilibrium. Intrinsic factors such as base sequence and covalent chemical modification of the base or of the backbone can also promote a right-handed B to left-handed Z transition. It has been reported that halogen substitution on the pyrimidine C5 position facilitates the B-Z transition (Malfoy et al., 1982). Methyl substitution of the pyrimidine C5 was shown to stabilize the Z form of alternating poly(dG-d5MeC) at physiological salt concentrations (Behe & Felsenfeld, 1981; Fujii et al., 1982). The efficiency of C5 substitution for stabilizing the left-handed form has been reported to increase in the order of iodo > bromo > methyl ≫ H (Jovin et al., 1983a). Bromination in the guanine C8 position also stabilizes Z-DNA (Moller et al., 1984), presumably by stabilizing the syn conformation present in the Z form.

The commonly used spectroscopic criteria, such as circular dichroism (CD), IR, Raman, and ^{31}P NMR spectra, however, cannot unambiguously define structure in solution. Another method of identifying the handedness of a DNA duplex is based on the immunogenicity of Z-DNA. Z-DNA elicits the production of antibodies specific for the left-handed form in a variety of organisms (Lafer et al., 1981; Malfoy & Leng, 1981; Moller et al., 1982; Pohl et al., 1982). Such antibodies have been used to show the existence of the Z form in native DNA by the use of immunofluorescence microscopy (Nordheim et al., 1981; Jovin et al., 1983a,b; Lemeunier et al., 1982; Lipps et al., 1983; Morgenegg et al., 1983; Arndt-Jovin et al., 1985a,b) and competitive radioimmunoassay (Lafer et al., 1981; Rich, 1983; Jovin et al., 1983c). It was reported, for example, that poly(d2NH$_2$A-dT) in preliminary experiments interacts at high ionic strength with antibodies specific for Z-DNA, and it was indicated that this polymer has the structural characteristics of left-handed Z-DNA under those conditions (Jovin et al., 1983a). Preliminary results on poly(d2NH$_2$A-dT) with CD and ^{31}P NMR also suggested a Z-like structure (Howard et al., 1984; Gaffney et al., 1982).

One-dimensional and two-dimensional nuclear Overhauser enhancement (1D and 2D NOE) spectroscopy provides a unique method for detailed conformational analysis of polydeoxynucleotides in solution (Assa-Munt & Kearns, 1984; Borah et al., 1985a,b). Recent work in this laboratory using 2D NOE spectroscopy has demonstrated that poly(d2NH$_2$A-dT) in high salt concentration adopts an A form or closely related structure (Borah et al., 1985b) rather than the Z form suggested in the reports cited above. The observed base proton-H3′ cross-peaks in the 2D NOE spectra indicated a 3′-endo sugar pucker for both the 2NH$_2$A and T nucleotides in an A conformation. This significant finding has prompted us to investigate two other alternating copolymers, poly(d2NH$_2$A-d5IU) and poly(d2NH$_2$A-d5BrU), using 1D and 2D NOE methods as well as CD and UV spectroscopy. We have analyzed the 1D and 2D NOE spectra of these polymers in low- and high-salt conditions and compared them with spectra characteristic of B, Z, and A forms (Borah et al., 1985b). Our conclusion is that both the poly(d2NH$_2$A-d5XU) copolymers also give an A form rather than a Z form in high salt. These results have consequences for the interpretation of anti-Z antibody binding to native DNA.

Materials and Methods

Materials. 5-Bromodeoxyuridine 5′-triphosphate (lot no. 769031), 5-iododeoxyuridine 5′-triphosphate (lot no. 867041), poly(dA-dT) (lot no. 658192), and DNA polymerase I from *Eschericia coli* (lot no. 926-10) were from Pharmacia. Synthesis of 2-aminodeoxyadenosine 5′-triphosphate has been

* Author to whom correspondence should be addressed.
‡ National Cancer Institute, National Institutes of Health.
§ National Institute of Arthritis, Diabetes and Digestive and Kidney Diseases, National Institutes of Health.